Discrete element modeling of ballast reinforced with triangular aperture geogrid

Yu Qian, Debakanta Mishra, & Erol Tutumluer,
University of Illinois at Urbana-Champaign, Urbana, Illinois, USA

Jayhyun Kwon
Tensar International Corporation, Inc., Alpharetta, Georgia, USA

ABSTRACT: Geogrids have been successfully used in railroad applications for ballast and sub-ballast stabilization purposes for many decades. When granular material is placed and compacted over the geogrid, aggregate particles interlock within the geogrid and are confined within the apertures. A triangular aperture geogrid was used to stabilize railroad ballast in this study. The performance of the stabilized ballast samples were evaluated in the laboratory using a large scale triaxial test device and strength testing of the geogrid-reinforced ballast samples. Both single and multiple layers of the triangular aperture geogrid were placed at different locations in test specimens to identify optimal application of geogrid for maximizing ballast strength properties. Interestingly, the highest strength was achieved when two triangular aperture geogrids were placed in mid-specimen lateral bulging zone. To further investigate the geogrid reinforcement mechanisms, an imaging based Discrete Element Modeling (DEM) approach was also adopted with the capability to create actual ballast aggregate particles as three-dimensional polyhedron elements having the same particle size distributions and imaging quantified average shapes and angularities. The DEM approach successfully predicted the measured strength properties of the geogrid-reinforced ballast specimens with the geogrids placed at different depths in the cylindrical test specimens.

KEY WORDS**:** Ballast, geogrid reinforcement, triaxial testing, discrete element modeling.

1 INTRODUCTION

Geogrids have been used in railroad track structures for stabilization and reinforcement purposes, especially for subgrade restraint and reinforcing subballast and ballast layers. In general, geogrid is placed on top of weak subgrade to bridge over soft soils with variable strength characteristics. Another benefit of using geogrid comes from the interlock established between large ballast particles and the geogrid to restrain lateral movement of ballast particles. Railroad ballast consists of large size angular aggregates with uniform gradation to facilitate drainage and load distribution. Fouling of ballast occurs due to mechanical wear of sharp edges and aggregate particle breakage through repeated loading. The inclusion of geogrid within ballast layer will limit lateral movement of ballast particles and reduce vertical settlement and thereby reduce ballast breakdown. For this purpose, geogrids can be placed within the ballast layer at different depths and locations. What dictates the geogrid location

within a ballast/subballast layer in the field is often the depth below which tamping arms or tines of ballast tamping equipment cannot reach during routine railroad maintenance activities.

Biaxial geogrids with rectangular or square apertures have tensile strength properties in both machine and cross-machine directions. These traditional geogrids have proven to be quite effective for improving bearing capacity of the track substructure by increasing ballast/subballast stiffness and reducing its permanent deformation under repeated train loading (Bathurst and Raymond 1987, Shin et al. 2002, Raymond and Ismail 2003, Indraratna et al. 2006, Brown et al. 2007, Kwon and Penman 2009, Qian et al. 2011a). Recently, geogrids with triangular aperture shapes are also being considered for ballast reinforcement with claims to possess superior benefits since they can provide improved reinforcement through geogrid-aggregate interlock in all directions. An early work on comparative modeling evaluation of the reinforcement benefits of geogrids with rectangular and triangular geogrids was offered by Tutumluer et al. (2009a) through discrete element modeling simulations of direct shear tests. More recent research efforts have focused on evaluating performance improvements of geogrid reinforced transportation systems and how to adequately investigate the related reinforcement mechanism through the geogrid-aggregate interlock (Qian et al. 2011b, Qian et al. 2012).

This paper describes preliminary findings from an ongoing research study at the University of Illinois with the aim to conduct monotonic strength testing of triangular aperture geogrid-reinforced ballast specimens using a large scale triaxial test device and model the micromechanical interlock behavior of geogrid-aggregate systems with the discrete element method. The triangular aperture geogrid-reinforced ballast specimens were tested under three different configurations to evaluate the reinforcement benefits through stress-strain behavior and strength properties. An unreinforced ballast specimen established the control test. To simulate the monotonic triaxial loading tests and investigate the geogrid reinforcement mechanisms, a numerical modeling approach based on Discrete Element Method (DEM) was adopted with the capability to create actual ballast aggregate particles as three-dimensional polyhedron elements having the same particle size distributions and imaging quantified average shapes and angularities. Both the large scale triaxial strength test and the DEM simulation results are presented to evaluate the reinforcement benefits and the mechanisms governing behavior of the ballast specimens reinforced with triangular aperture geogrids.

2 TRIAXIAL STRENGTH TESTS OF BALLAST SPECIMENS

2.1 The University of Illinois triaxial ballast tester (TX-24)

A large scale triaxial test device (The University of Illinois Triaxial Ballast Tester or TX-24) was recently developed at the University of Illinois for testing specifically ballast size aggregate materials. The test specimen dimensions are 30.5 cm (12 in.) in diameter and 61.0 cm (24 in.) in height. The acrylic test chamber has dimensions of 61.0 cm (24 in.) in diameter and 122.0 cm (48 in.) in height. An internal load cell (Honeywell Model 3174) with a capacity of 89 kN (20 kips) is placed on top of the specimen top platen. Three vertical LVDTs are placed around the cylindrical test specimen at 120-degree angles between each other to measure the vertical deformations of the specimen from three different side locations. Another LVDT is mounted on a circumferential chain wrapped around the specimen at the mid-height to measure the radial deformation of the test specimen. Figure 1 shows a photo of the TX-24 setup having an instrumented ballast specimen ready for testing.

Garg and Thompson (1997) evaluated strength properties of granular materials under transportation vehicle loading at rather rapid monotonic loading rates of the ram moving up to a maximum displacement of 38 mm (1.5 in.) per second. In this study, with the intent to also investigate the influence of higher traffic induced loading rate on the large scale triaxial strength test results of ballast materials, laboratory tests were conducted at a rapid shear rate of 5% strain per second with a constant confining pressure of 137.8 kPa (20 psi). Considering the 61.0-cm (24-in.) high ballast specimen, these loading rates correspond to vertical ram movements of 30.5 mm (1.2 in.) per second and in order not to damage the circumferential chain and the LVDTs during the large movements of the ram causing instant bulging and shearing of ballast samples, the LVDTs were not used during the ballast strength tests.

Figure 1: The University of Illinois triaxial ballast tester (TX-24)

2.2 Ballast Specimen Preparation

The ballast material used in the triaxial strength tests was a clean limestone having 100% crushed aggregates. Figure 2 shows the gradation properties of the ballast material which adequately met the US AREMA No. 24 gradation requirements. Besides the grain size distribution, aggregate shape properties, especially the flat and elongated (F&E) ratio, the angularity index (AI), and the surface texture (ST) index, are key indices quantified by the recently enhanced University of Illinois Aggregate Image Analyzer (UIAIA) (Rao et al. 2002). One full bucket of the ballast material was scanned and analyzed using the UIAIA to determine the values of the F&E ratio, AI, and ST index. These shape indices were then used as the essential morphological data to generate ballast aggregate particle shapes as three-dimensional (3D) polyhedrons, i.e., individual discrete elements utilized in the ballast DEM model (see Figure 3).

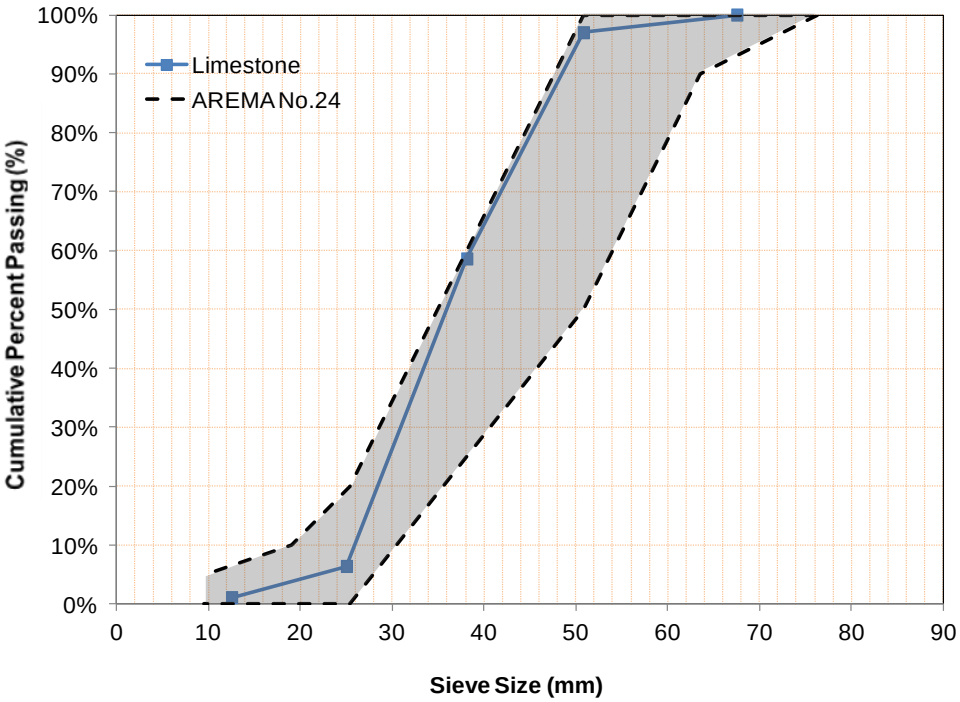

Figure 2: Particle size distribution of limestone ballast aggregate compared to AREMA No. 24 specifications

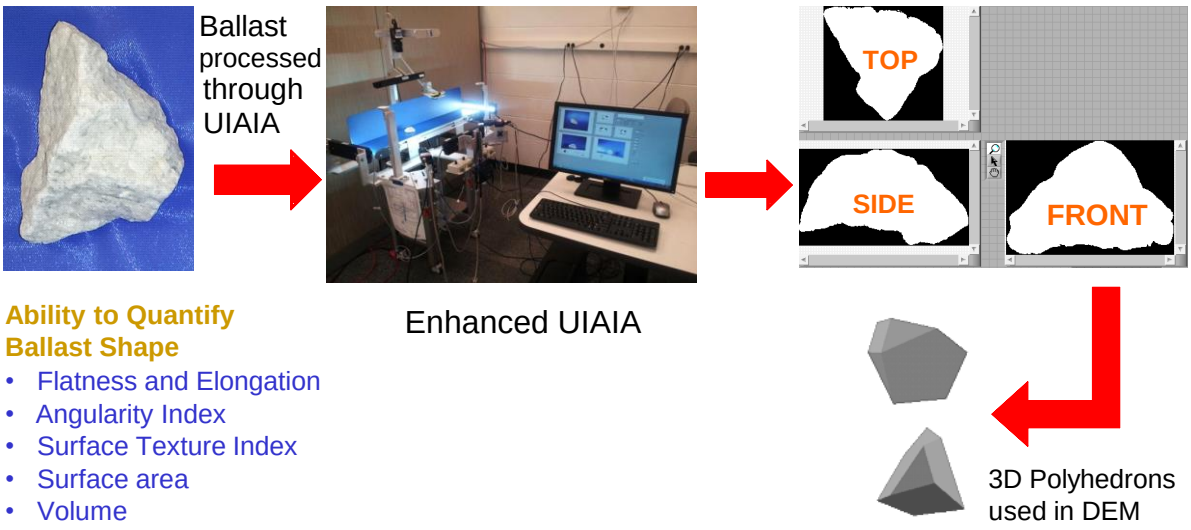

Figure 3: Conceptual approach for aggregate imaging based railroad ballast discrete element model simulations

An aluminum split mold was used to prepare the ballast test specimens. Three layers of latex membrane, with a total thickness of 2.3 mm, were fixed inside the split mold and held in place by applying vacuum to prepare each specimen in layers. A thin layer of geotextile was placed on top of the base plate to prevent clogging of the vacuum port in the base plate. Approximately 68 to 73 kg (150 to 160 lbs) of ballast material was poured into the mold in several lifts, with each lift compacted approximately 15-cm to 25-cm (6-in. to 10-in) high. Each lift was compacted using a 27.2 kg (60 lbs) electric jack hammer for about 4 to 6 seconds. The thickness of each lift and corresponding compaction time were calculated to ensure even compaction based on where geogrid was placed. After compaction of specimen

to desired depth, geogrid was placed into the test specimen. Figure 4 shows the photo of the triaxial aperture geogrid used in this study. At the end of placing all lifts and geogrid(s), each test specimen was checked for the total height and leveling of the top plate. The void ratios (e) computed were consistently around 0.68. Figure 5 demonstrates the different configurations, i.e., locations where geogrid was placed. Although placing two layers of geogrid within ballast is not often practical and may not be cost effective in the field, the two layers of geogrids installed in the test specimens were intended to investigate in the laboratory and through DEM modeling the aggregate-geogrid interlock mechanism for preventing sample bulging. Detailed properties of the triangular aperture geogrid, the gradation properties and the average values of the limestone ballast UIAIA shape indices are given in Table 1.

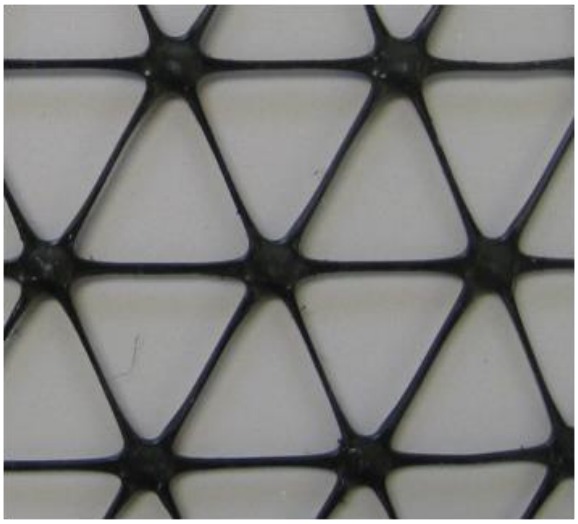

Figure 4: Triangular aperture geogrid used in large scale triaxial tests

Table 1: Properties of limestone ballast aggregate and triangular aperture geogrid used

Limestone Properties				
Angularity Index (AI) in degrees	Flat & Elongation (F&E) Ratio	Surface Texture (ST)	Cu	Cc
440	2.3	2	1.46	0.97
Triangular Aperture Geogrid Properties				
Aperture Dimensions (mm)		Longitudinal	Diagonal	
		60	60	
Mechanical Properties				
Junction Efficiency (percentage)		93		
Radial stiffness (kN/m@0.5% strain)		350		

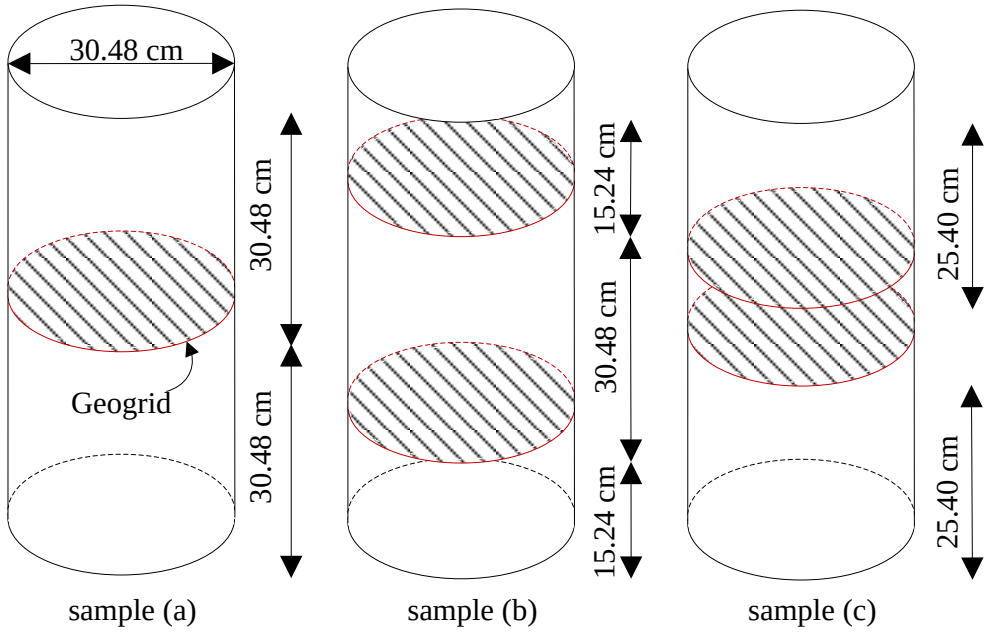

Figure 5: Different configurations used in large scale triaxial tests with geogrid reinforcement

3 SIMULATION OF TRIAXIAL TEST USING THE DISCRETE ELEMENT METHOD

3.1 DEM model preparation

To investigate the mechanism of interlock and how this minimizes particle movement and causes local stiffness increasing through interaction of ballast particles with geogrid, a numerical modeling approach was adopted based on the Discrete Element Method (DEM) combined with image analyses of tested aggregate particles for particle size and shape properties. Compared to other research studies focusing on simulating triaxial tests by DEM, which often use spherical elements or element clusters (Indraratna et al. 2010, Lu and McDowell 2010), the image-aided DEM simulation approach developed at the University of Illinois has the capability to create actual ballast aggregate particles as 3D polyhedron elements having the same particle size distributions and imaging quantified average shapes and angularities. Ghaboussi and Barbosa (1990) developed the first polyhedral 3D DEM code BLOKS3D for particle flow; and Nezami et al. (2006) enhanced the program with new, fast contact detection algorithms.

Tutumluer et al. (2006) combined the DEM program and the aggregate image analysis together to simulate the ballast behavior more accurately and realistically by using these polyhedral elements regenerated from the image analysis results of ballast materials. This DEM approach was first calibrated by laboratory large scale direct shear test results for ballast size aggregate application (Tutumluer et al. 2006). The calibrated DEM model was then utilized to model strength and settlement behavior of railroad ballast for the effects of multi-scale aggregate morphological properties (Tutumluer et al. 2006, 2007). More recent applications of the calibrated DEM model investigated ballast gradation (Tutumluer et al. 2009b) and fouling issues (Tutumluer et al. 2008, Huang and Tutumluer 2011) that are known to influence track performance. A successful field validation study was conducted with the ballast DEM simulation approach through constructing and monitoring field settlement records of four different ballast test sections and then comparing the measured ballast

settlements under monitored train loadings to DEM model predictions (Tutumluer et al. 2011). The effect of geogrid aperture size was also successfully studied by this DEM approach (Qian et al. 2011a).

To simulate large scale triaxial compression tests using the DEM approach, the first challenge is to model the membrane which holds the specimen upright and applies the chamber confining pressure on it during testing. Previous modeling studies used rigid boundaries and chains of circular or spherical particles to simulate the membrane (Bardet 1994, Iwashita and Oda 2000, Markauskas and Kacianauskas 2006, Wang and Tonon, 2009). Lee et al. (2012) recently used rigid rectangular cuboid discrete elements positioned in a cylindrical arrangement to simulate a flexible membrane with BLOKS3D. A similar approach was used in this study.

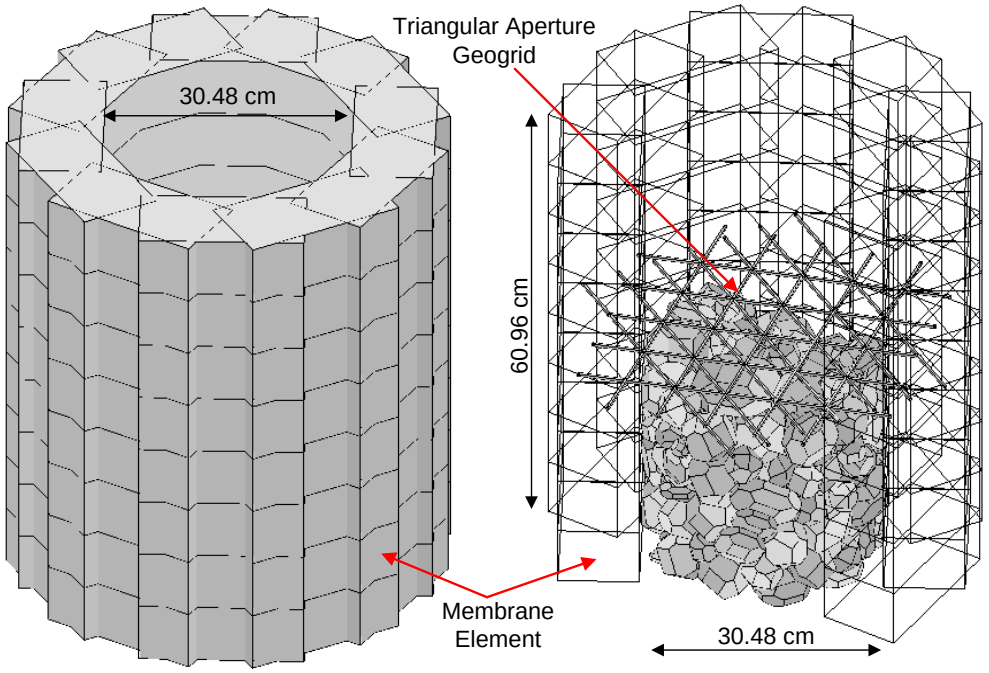

Figure 6: Flexible membrane, one layer of geogrid and ballast specimen formed in DEM simulations

A total of 96 rectangular cuboid discrete elements (in eight-layers) were used to form a cylindrical chamber to confine the ballast specimen as shown in Figure 6. Each layer had 12 equal size elements and the dimension of each single element was 20.32 cm (8 in.) long, 10.16 cm (4 in.) wide, and 7.62 cm (3 in.) high. These membrane elements were only allowed translational movement in radial direction. Rotation and translation movement in other directions were restricted to replicate the deformation of membrane. Note that these elements were required to have certain thickness to avoid any gap between adjacent layers when differential radial displacements between them were relatively large. Similarly, the elements were also allowed to have sufficient lengths to overlap adjacent elements to keep the circular chamber closed during simulation of triaxial tests. No contact detection was performed between these elements to allow for each element to move freely, independent of neighboring elements. The friction between the membrane elements and the ballast particles in contact with them was ignored during the DEM simulations. For the unreinforced ballast specimen, after the membrane was formed, around 500 particles were poured into the cylinder and the top platen was placed on top of the specimen to compact the ballast specimen to the same initial density under 137.8 kPa (20 psi) confining pressure as achieved in the laboratory

experiment. For the geogrid reinforced ballast specimens, after the membrane was formed, about 500 particles were also poured into the cylinder by layers the same as the experiment procedures, while in between, geogrid elements were generated in the desired height of the ballast specimen as shown in Figure 6. When the ballast specimen in the DEM simulation was prepared as in the same condition as the laboratory test specimen, the top platen was moved down at the same strain rate (5% per second) of the experiments to start the strength test.

4 LABORATORY TESTS AND DEM SIMULATION RESULTS

Figure 7 presents the results of the large scale triaxial strength tests on the limestone ballast cylindrical specimens for up to 10% axial strain. All the test specimens showed similar stress-strain behavior at the initial small strain stage of the strength tests and this was primarily due to the fact that geogrids were not yet fully mobilized early on. When axial strain levels increased, the geogrid was mobilized and the interlock between geogrid and aggregate particles prevented movement or specimen bulging. The zigzag shapes of the stress-strain curves at high axial strain levels indicate sudden strength drops. This can be explained by damaged geogrid due to observed broken ribs and/or particles reorienting themselves from the interlocked position. Immediately afterwards, the geogrid-reinforced ballast was back to fully restrained condition again with new interlock between aggregate particles and the geogrid formed and the strength of the specimen restored upon completion of the particle rearrangement.

The location the geogrid is placed within the specimen can be referred to as the "stiffened or reinforced" zone due to the significant interaction of geogrid and aggregates (Qian et al 2011a). As expected, geogrid placed at different specimen heights produced distinct reinforcement configurations by creating these different "stiffened or reinforced" zones. Considering that the most severe bulging took place in the mid-specimen height for the unreinforced ballast sample, when the geogrid was placed in the mid-specimen height, the reinforcement effect was quite significant especially when large axial strains were reached. For the double layer geogrid application, two geogrids were placed at 25.4 cm (10 in.) from the bottom and top of the specimen, respectively. The lateral movement or bulging in the middle 10.2-cm (4-in.) specimen length between the two layers of geogrid was effectively arrested and a "stiffened or reinforced" zone was formed due to the interlock between aggregates and geogrids to result in the highest ballast sample strength achieved (see Figure 7). Accordingly, the ballast sample with two layers of geogrid placed at 25.4 cm (10 in.) from the bottom and top of the specimen presented the best performance from the experiments when compared to other configurations including a single layer geogrid placed in mid-specimen height. However, when geogrids were placed at 15.24 cm (6 in.) from the top and bottom or a single layer of geogrid placed at 15.24 cm (6 in.) from the top or bottom, the reinforcement effect was not as good as single layer of geogrid place at the middle or double layers of geogrid placed at 25.4 cm (10 in.) from the top and bottom of the specimen.

This is because the critical location, i.e., the middle of the specimen, could not be effectively reinforced if the geogrid was placed too far away. These were the conditions when the shear plane was pushed towards the unreinforced region of the ballast specimen to fail the ballast sample. Hence, no significant strength improvement was observed even when two layers of geogrid were placed at 25.4 cm (10 in.) from the top and bottom of the specimen when compared with the unreinforced specimen strength properties.

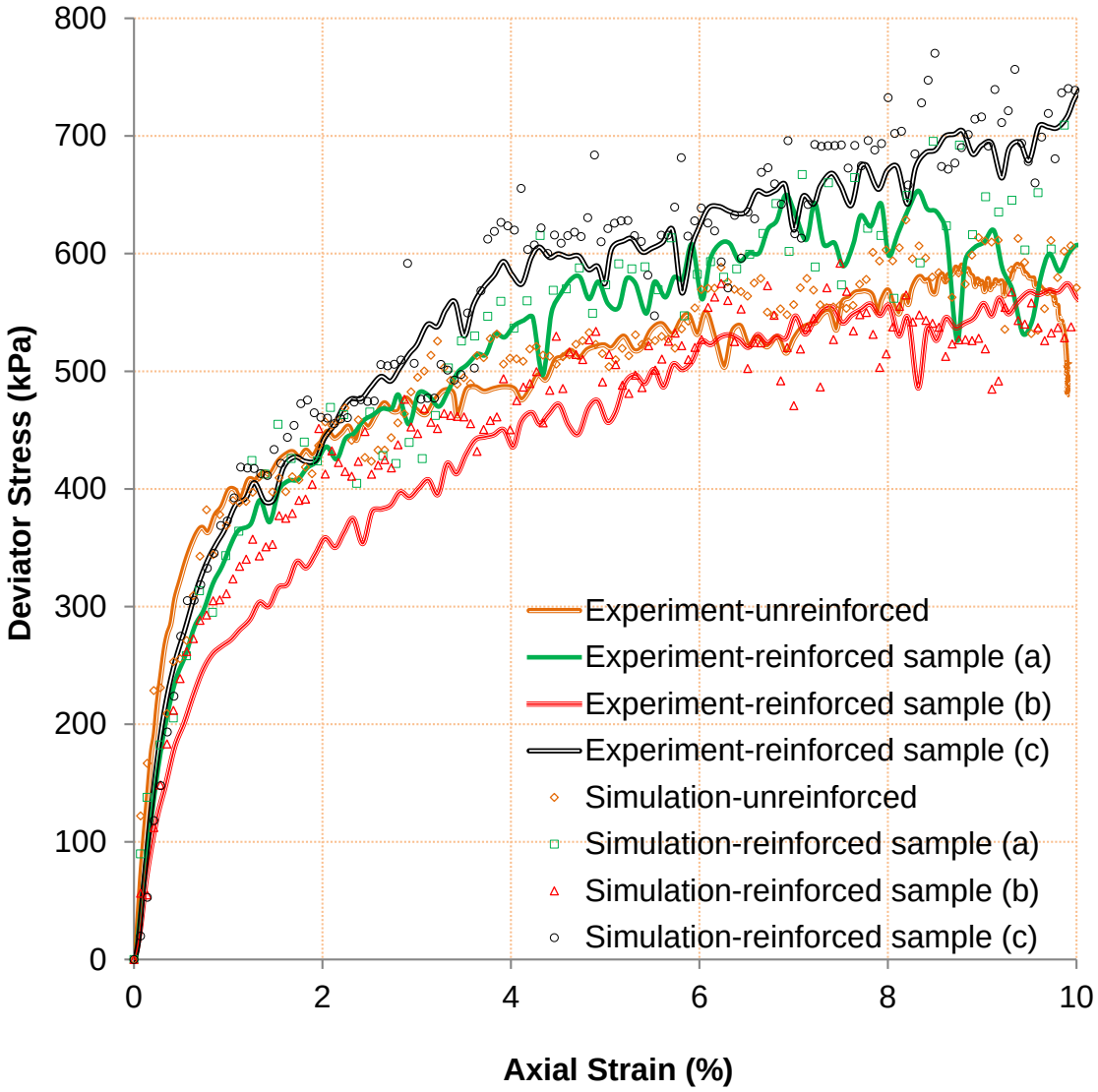

Figure 7. Laboratory large scale triaxial ballast strength tests and DEM simulation results

5 CONCLUSIONS

This paper focused on the strength test results of geogrid reinforced ballast specimens as obtained from a large scale triaxial test device in the laboratory and triangular aperture geogrids used for ballast reinforcement. The goal was to demonstrate the applicability of an aggregate particle imaging based three-dimensional (3-D) numerical modeling approach, based on the Discrete Element Method (DEM), for studying geogrid-aggregate interlock reinforcement mechanism in the case of ballast reinforcement with triangular aperture geogrids and the optimal reinforcement location of cylindrical test specimens in order to maximize strength properties. The following conclusions can be drawn from this study:

- The location of geogrid placement in a uniform sized aggregate assembly, such as railroad ballast, influences significantly the stress-strain behavior of cylindrical test specimen through creating different local "stiffened zones" and therefore reinforcement effects. Placing a single layer of geogrid at mid-specimen height, or two layers of geogrid close to

the middle of the specimen where bulging takes place, provides better reinforcement benefits when compared to placing geogrid towards top and bottom, i.e., away from the middle of the test specimen, during triaxial strength testing.

- The aggregate imaging based DEM simulation platform developed at the University of Illinois could model the stress-strain behavior of ballast specimens under monotonic loading triaxial strength tests. The DEM simulation successfully captured the stress-strain behavior trends of the geogrid-reinforced ballast specimens by addressing adequately the initial condition of the laboratory tests. The DEM simulation platform currently being further developed has the potential for quantifying individual effects of various geogrid properties, such as aperture shape and size and rib dimensions, on the aggregate assembly.

6 ACKNOWLEDGEMENTS

The authors would like to acknowledge Tensar International, Inc. for providing the triangular aperture geogrids studied. The help and support of Mr. James Pforr, Research Engineer at the Illinois Center for Transportation (ICT) and Mr. Hasan Kazmee, PhD student at the Department of Civil and Environmental Engineering (CEE) at UIUC with the laboratory triaxial tests are greatly appreciated.

REFERENCES

Bardet, J. P., 1994. *Observations on the Effects of Particle Rotations on the Failure of Idealized Granular Materials*. Mechanics of materials, 18(2):159-182.

Bathurst, R. J. and Raymond, G. P., 1987. *Geogrid Reinforcement of Ballasted Track*. Transportation Research Record. No. 1153: 8-14.

Brown, S. F., Kwan, J. and Thom, N. H., 2007. *Identifying the Key Parameters that Influence Geogrid Reinforcement of Railway Ballast*. Geotextiles and Geomembranes, 25(6):326-335.

Garg, N. and Thompson, M.R., 1997. *Triaxial Characterization of Minnesota Road Research Project Granular Materials*. Journal of the Transportation Research Board. No.1577:27-36.

Ghaboussi J. and Barbosa R., 1990. *Three-dimensional Discrete Element Method for Granular Materials*. International Journal for Numerical and Analytical Methods in Geomechanics, (14): 451-472.

Huang H., and Tutumluer E., 2011. *Discrete Element Modeling for Fouled Railroad Ballast*. Construction and Building Materials, (25): 3306‐3312.

Indraratna, B., Khabbaz, H., Salim, W. and Christie, D., 2006. *Geotechnical Properties of Ballast and the Role of Geosynthetics in Rail Track Stabilisation*. Journal of Ground Improvement, 10(3): 91-102.

Indraratna, B., Thakur, P.K., and Vinod, J.S., 2010. *Experimental and Numerical Study of Railway Ballast Behavior under Cyclic Loading*. International Journal of Geomechanics, ASCE, 10(4):136-144.

Iwashita K., and Oda M., 2000. *Micro-deformation Mechanism of Shear Banding Process Based on Modified Distinct Element Method*. Powder Technology, 109(1-3):192-205.

Lee, S. J., Hashash, Y.M.A., and Nezami E.G., 2012. *Simulation of Triaxial Compression Test with Polyhedral Discrete Elements*. Computers and Geotechnics, in press.

Lu, M. and McDowell, G.R., 2010. *Discrete Element Modelling of Railway Ballast under Monotonic and Cyclic Triaxial Loading*. Geotechnique, 60(6):459-467.

Kwon, J. and Penman, J., 2009. *The Use of Biaxial Geogrids for Enhancing the Performance of Sub-Ballast and Ballast Layers—Previous Experience and Research*. 8th International

Conference on Bearing Capacity of Roads, Railways and Airfields. June 29-July 2, Champaign, Illinois, USA.

Markauskas D. and Kacianauskas R., 2006. *Compacting of Particles for Biaxial Compression Test by the Discrete Element Method*. Journal of Civil Engineering and Management, 12(2):153-61.

Nezami E.G., Hashash, Y.M.A., Zhao D., Ghaboussi J., 2006. *Shortest Link Method for Contact Detection in Discrete Element Method*. International Journal for Numerical and Analytical Methods in Geomechanics, 30(8):783-801.

Qian, Y., Tutumluer, E., and Huang, H., 2011a. *A Validated Discrete Element Modeling Approach for Studying Geogrid-Aggregate Reinforcement Mechanisms*. Geo-Frontiers 2011, ASCE Geo-Institute, March 13-16, Dallas, Texas.

Qian, Y., Han, J., and Pokharel, S.K., and Parsons, R.L., 2011b. *Stress Analysis on Triangular Aperture Geogrid-Reinforced Bases over Weak Subgrade under Cyclic Loading - An Experimental Study*. Journal of the Transportation Research Board, No. 2204, Low-Volume Roads, Vol. 2, Proceedings of the 10th International Conference on Low-Volume Roads, July 24–27, Lake Buena Vista, Florida, USA, 83-91.

Qian, Y., Han, J., and Pokharel, S.K., and Parsons, R.L., 2012. *Performance of Triangular Aperture Geogrid-Reinforced Base Courses over Weak Subgrade under Cyclic Loading*. Journal of Materials in Civil Engineering, in press.

Rao, C., Tutumluer, E. and Kim, I.T., 2002. *Quantification of Coarse Aggregate Angularity Based on Image Analysis*. Transportation Research Record. No. 1787, 193-201.

Raymond, G. and Ismail, I., 2003. *The Effect of Geogrid Reinforcement on Unbound Aggregates*. Geotextiles and Geomembranes, 21(6): pp.355-380.

Shin, E. C., Kim, D. H. and Das, B. M., 2002. *Geogrid-Reinforced Railroad Bed Settlement Due to Cyclic Load*. Geotechnical and Geological Engineering, 20:261-271.

Tutumluer, E., Huang, H., Hashash, Y.M.A., and Ghaboussi, J., 2006. *Aggregate Shape Effects on Ballast Tamping and Railroad Track Lateral Stability*. In Proceedings of the AREMA Annual Conference, Louisville, Kentucky, USA, September 17-20.

Tutumluer, E., Huang, H., Hashash, Y.M.A., and Ghaboussi, J., 2007. *Discrete Element Modeling of Railroad Ballast Settlement*. In Proceedings of the AREMA Annual Conference, Chicago, Illinois, September 9-12.

Tutumluer, E., Huang, H., Hashash, Y.M.A., and Ghaboussi, J., 2008. *Laboratory Characterization of Coal Dust Fouled Ballast Behavior*. In Proceedings of the AREMA Annual Conference, Salt Lake City, Utah, September 21-23.

Tutumluer, E, Huang, H., and Bian, X. 2009a. *Research on the Behavior of Geogrids in Stabilization Applications*, Proc., Jubilee Symposium on Polymer Geogrid Reinforcement, September 8, 2009, London, UK.

Tutumluer, E., Huang, H., Hashash, Y.M.A., and Ghaboussi, J., 2009b. *AREMA Gradations Affecting Ballast Performance Using Discrete Element Modeling (DEM) Approach*. In Proceedings of the AREMA Annual Conference, Chicago, Illinois, September 20-23.

Tutumluer, E., Qian, Y., Hashash, Y.M.A., Ghaboussi, J., and David, D.D., 2011. *Field Validated Discrete Element Model for Railroad Ballast*. In Proceedings of the AREMA Annual Conference, Minneapolis, Minnesota, September 18-21.

Wang, Y. and Tonon, F., 2009. *Modeling Triaxial Test on Intact Rock Using Discrete Element Method with Membrane Boundary*. Journal of Engineering Mechanics, 135(9):1029-1037.